
This is the **accepted version** of the journal article:

Spiekman, Stephan N. F.; Muijal, Eudald. «Decapitation in the long-necked Triassic marine reptile Tanystropheus». *Current Biology*, (June 2023). DOI 10.1016/j.cub.2023.04.027

This version is available at <https://ddd.uab.cat/record/276577>

under the terms of the  license

Decapitation in the long-necked reptile *Tanystropheus* (Archosauromorpha, Tanystropheidae)

Stephan N. F. Spiekman^{1,3,4,*} and Eudald Muiàl^{1,2,3,*}

¹Staatliches Museum für Naturkunde Stuttgart; Stuttgart, D-70191; Germany

²Institut Català de Paleontologia Miquel Crusafont; Cerdanyola del Vallès, Catalonia, E-08193; Spain

³The authors contributed equally

⁴Lead contact

*Correspondence: stephanspiekman@gmail.com, eudald.muiàlgrane@smns-bw.de

Twitter handle: @StephanSpiekman

Extreme neck elongation was a common evolutionary strategy among Mesozoic marine reptiles, occurring independently in several lineages^{1,2}. Despite its evolutionary success, such an elongate neck might have been particularly susceptible to predation (e.g.¹), but direct evidence for this interpretation has been lacking until now. Composed of 13 hyperelongate vertebrae and associated strut-like ribs, the long neck of the Triassic archosauromorph *Tanystropheus* represents a unique structure among tetrapods. It was likely stiffened and used to catch prey through an ambush-strategy². Here, we show that the neck was completely severed in two *Tanystropheus* specimens (Figure 1), most likely due to a predatory attack, providing vivid evidence of predator-prey interactions among Mesozoic marine reptiles that are rarely preserved in the fossil record. The recurring incidence of decapitation suggests that the elongate neck represented a functional weak spot in *Tanystropheus*, and possibly the long-necked marine reptile *bauplan* generally.

The *Tanystropheus* specimens (PIMUZ T 2819: *T. hydroides*; PIMUZ T 3901: *T. longobardicus*) derive from the Middle Triassic marine fossil lagerstätte of Monte San Giorgio² (Supplemental Information). Both preserve a complete skull and an incomplete cervical column, which abruptly terminates at a distinct break in a vertebra and its associated ribs (Figure 1A, B; Figure S1). The fractures of the broken vertebrae of both specimens are generally oblique and spiral, and they display smooth surfaces, corresponding to fractures produced on fresh bones in the perimortem phase (i.e. at or shortly after death³).

PIMUZ T 2819 only possesses bite traces (two punctures and a score, *sensu*⁴) on the 10th vertebra adjacent to the break (Figure 1C-E; Figure S1A). The punctures are aligned and accompany the broken section of the neck, suggesting that they are directly related to the decapitating bite. This bite caused a major fracture within the vertebra, which formed a large V-shaped bone splinter (*sensu*³). The score, positioned on the V-shaped splinter, is not directly aligned with these other bite

traces (Figure 1D, E), indicating a prior bite in the same region of the vertebra. Based on the posteriorly widening score, the movement of the tooth tracing the bone was backwards with respect to the vertebra: after grasping the neck, the predator pulled back (as observed in certain reptilian predators⁵). Considering also the back and upwards-displaced V-shaped splinter, and the broken posterior end of the dorsal puncture, the neck was most likely bitten from above and the rear. Thus, from this approach angle, the neck of PIMUZ T 2819 was bitten at least twice in close succession, with the final bite severing the neck.

The nature of the break in the 7th vertebra in PIMUZ T 3901 (Figure 1F; Figure S1B), with splintering of the bone (*sensu*³), indicates that this neck was also severed by a violent bite. In addition, an oval pit (*sensu*⁴) on the dorsolateral side of the posterior part of the 5th vertebra (Figure 1G; Figure S1C) and a corresponding breakage of an accompanying rib (Figure 1H) clearly suggest this part of the neck was also bitten, possibly representing an initial attack, with the predator coming from above as in PIMUZ T 2819.

While the fractures observed on the broken vertebrae resemble those occurring on fresh bones from violent impact³, the rest of the specimens remained intact, only showing decay features occurring in low energetic conditions (Supplemental Information). Although differentiating between predation and scavenging in the fossil record is notoriously difficult (e.g.⁶), several features support the former interpretation. Typical indications of scavenging, such as disarticulation plus scattering and destruction of elements, as well as numerous bite traces on bones^{5,6}, are all absent. Instead, all elements, including the delicate ribs, remain intact, being only broken in association with the bite traces. Furthermore, well-defined punctures inflicted by large predators, completely piercing the bone, as in PIMUZ T 2819 are often associated with predatory behaviors rather than scavenging (e.g.⁷). The predators most likely fed on the body posterior to the severed neck, which would have provided considerable nutrients contrary to the slender neck and head⁶, which were not consumed but instead abandoned.

The neck is severed near the posterior end of the 10th vertebra in PIMUZ T 2819 and at the base of the 7th vertebra in PIMUZ T 3901. In both *Tanystropheus* species, cervical vertebrae 7 to 10 are the longest, representing the mid-section of the neck. This region likely represented an optimal target for predators, since it is far away from the head yet anterior to the thicker and more muscular base of the neck⁸. The recurring decapitation in the mid-section of the neck in *Tanystropheus* might indicate preferential targeting by predators, but such a hypothesis remains tentative based on the limited available sample size.

Many predators could have inflicted the trauma to the comparatively small PIMUZ T 3901, including a medium-sized marine reptile with pointed dentition or a predatory fish. A similar

scenario was hypothesized for the holotype of *Macrocnemus obristi*, a similar-sized tanystropheid with a severed torso coming from geographically and temporally comparable deposits⁹. Fewer predators could have produced enough force to decapitate PIMUZ T 2819. Among the sufficiently large aquatic and terrestrial predators known from Monte San Giorgio, the 14.5 mm distance between the two punctures only corresponds to the known tooth spacing in the predatory marine reptiles *Nothosaurus giganteus*, *Cymbospondylus buchseri*, and *Helveticosaurus zollingeri*¹⁰. Consequently, the attack most likely occurred underwater, corresponding to a predominantly aquatic lifestyle inferred for *Tanystropheus hydroides* (Figure S2)².

Decapitation of both specimens corroborates that the long neck of *Tanystropheus* was slender and shows that it represented a vulnerable spot for predators. Perhaps *Tanystropheus* minimized encounters with larger predators by preferentially inhabiting the benthos of shallow aquatic environments and areas with limited visibility, also maximizing its own ambush-based predatory strategy. Despite being represented by a wealth of specimens and achieving comparable neck elongation, there is no unambiguous evidence for predatory targeting of long necks among plesiosaurs¹.



85
 86 **Figure 1. Decapitated specimens of *Tanystropheus*.** (A, C, D, E) *T. hydroides* (PIMUZ T 2819). (B, F, G,
 87 *T. longobardicus* (PIMUZ T 3901). (A, B) Overview of the specimens with the cervical vertebrae
 88 exposed on their left side; arrows in (B) point to the fractured vertebra and ribs, which are all broken
 89 in the same plane. (C) Detail of the broken vertebra (with a V-shaped bone splinter with the acute
 90 end pointing anteriorly, outlined with a white dashed line) and ribs; arrows highlight the alignment

of the severed vertebra and ribs. (D) Detail of the V-shaped bone splinter, bite traces including a score (grey arrow and interpretative outline), puncture (left black arrow), puncture that is open-ended posteriorly likely as a result of the pullback of the predator (right black arrow), and a vertical fracture (white arrow). (E) Detail of the score. (F) Detail of the broken vertebra and ribs, which are outlined by oblique and spiraled fractures with a smoothed broken surface in cross section. (G) Pit (arrowed). (H) Broken ribs (white arrows) likely associated with the bite trace in (G) (black arrow). Additional images and interpretative drawings of the bite traces and fractures are presented in Figure S1.

SUPPLEMENTAL INFORMATION

Supplemental Information includes supplemental methods, discussion and two figures, and can be found with this article online at [\[insert DOI\]](#).

Acknowledgments

We thank Christian Klug and Torsten Scheyer (PIMUZ) for specimen access, Adam Rytel (University of Warsaw) for additional photos of PIMUZ T 2819, and Torsten Scheyer, Adam Rytel, and Erin Maxwell (Staatliches Museum für Naturkunde Stuttgart) for discussions. We thank Roc Olivé (Institut Català de Paleontologia Miquel Crusafont) for producing the artwork in Figure S2, supported by a project of the Fundación Española para la Ciencia y la Tecnología - Ministerio de Ciencia e Innovación (Spanish Government). S.N.F.S. is supported by the Deutsche Forschungsgemeinschaft (grant no. SCHO 791/7-1 to R.R. Schoch), and E.M. by the CERCA program from Generalitat de Catalunya. We thank Valentin Fischer and three anonymous reviewers for constructive comments that helped to improve previous versions of the manuscript, as well as the editor Florian Maderspacher for handling the manuscript.

Author Contributions

S.N.F.S. and E.M. designed the study, performed the research, discussed the results, and wrote the manuscript and supplemental information. E.M. made Figure 1 and Figure S1. Both authors reviewed a final draft of the manuscript.

Declaration of Interests

The authors declare no competing interests.

REFERENCES

1. Noè, L.F., Taylor, M.A., and Gómez-Pérez, M. (2017). An integrated approach to understanding the role of the long neck in plesiosaurs. *Acta Palaeontologica Polonica* 62, 137-162.

2. Spiekman, S.N.F., Neenan, J.M., Fraser, N.C., Fernandez, V., Rieppel, O., Nosotti, S., and Scheyer, T.M. (2020). Aquatic habits and niche partitioning in the extraordinarily long-necked Triassic reptile *Tanystropheus*. *Current Biology* 30, 1-7.
3. Green, A.E., and Schultz, J.J. (2017). An examination of the transition of fracture characteristics in long bones from fresh to dry in central Florida: evaluating the timing of injury. *Journal of forensic sciences* 62, 282-291.
4. Binford, L.R. (1981). *Bones: ancient men and modern myths*, (San Diego, California, USA: Academic press).
5. Drumheller, S.K., and Brochu, C.A. (2016). Phylogenetic taphonomy: A statistical and phylogenetic approach for exploring taphonomic patterns in the fossil record using crocodylians. *Palaios* 31, 463-478.
6. Drumheller, S.K., McHugh, J.B., Kane, M., Riedel, A., and D'Amore, D.C. (2020). High frequencies of theropod bite marks provide evidence for feeding, scavenging, and possible cannibalism in a stressed Late Jurassic ecosystem. *PLoS One* 15, e0233115.
7. Fiorelli, L.E. (2010). Predation bite-marks on a peirosaurid crocodyliform from the Upper Cretaceous of Neuquén Province, Argentina. *Ameghiniana* 47, 387-400.
8. Tschanz, K. (1986). Funktionelle Anatomie der Halswirbelsäule von *Tanystropheus longobardicus* (Bassani) aus der Trias (Anis/Ladin) des Monte San Giorgio (Tessin) auf der Basis vergleichend morphologischer Untersuchungen an der Halsmuskulatur rezenter Echsen. PhD thesis Universität Zürich.
9. Fraser, N.C., and Furrer, H. (2013). A new species of *Macrocnemus* from the Middle Triassic of the eastern Swiss Alps. *Swiss Journal of Geosciences* 106, 199-206.
10. Rieppel, O. (2019). *Mesozoic Sea Dragons: Triassic Marine Life from the Ancient Tropical Lagoon of Monte San Giorgio*, (Bloomington, Indiana, USA: Indiana University Press).

SUPPLEMENTAL INFORMATION

Supplemental Figures

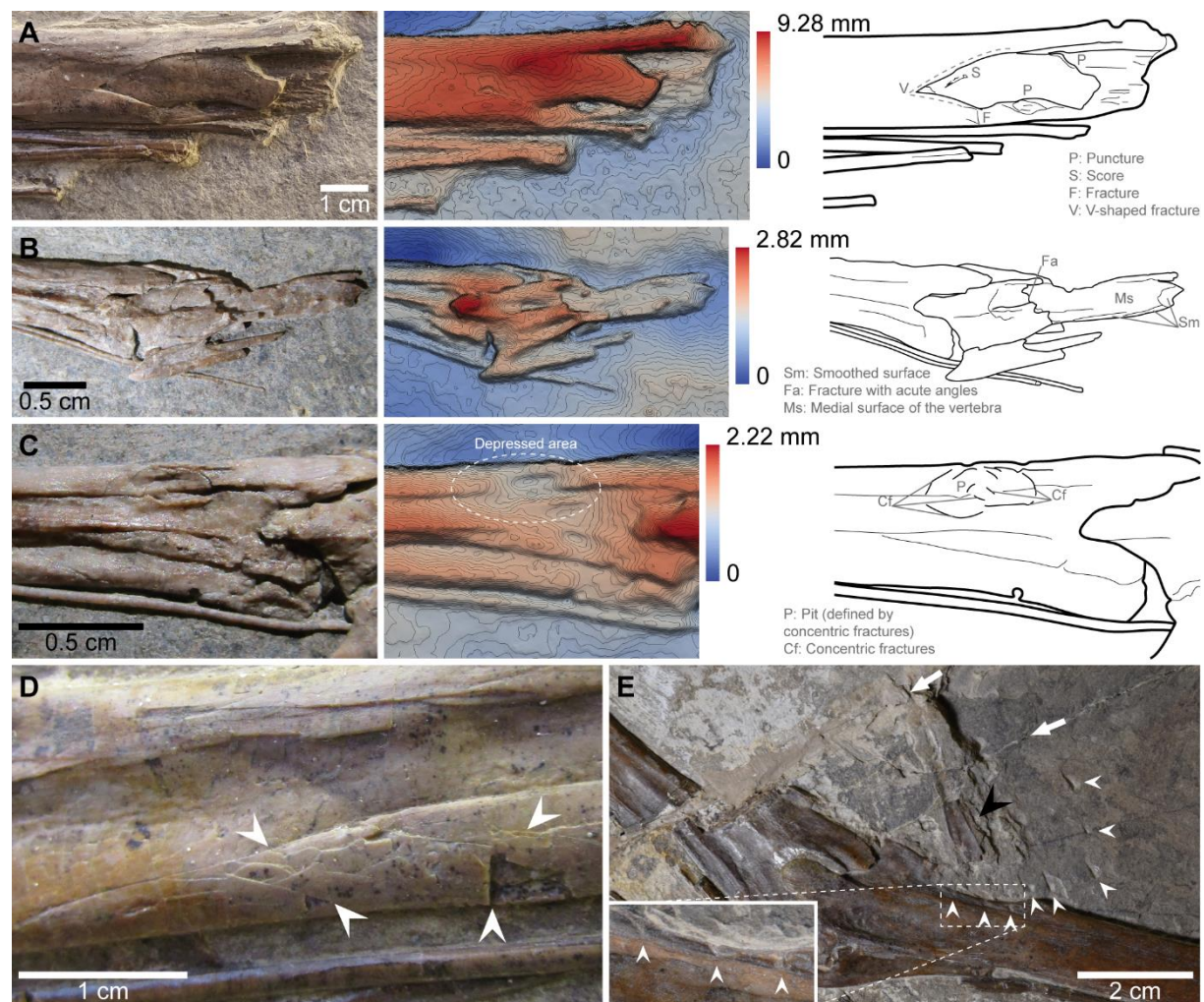


Figure S1. Details of bite traces and fractures. (A, B, C). Overview and interpretation of the fractures and bite traces in PIMUZ T 2819 (A), 7th vertebra of PIMUZ T 3901 (B) and 5th vertebra of PIMUZ T 3901 (C); (A, B, C) include photos of the specimen (left), false-color depth maps with contours obtained from the 3D photogrammetric models (middle) and interpretative outlines (right); the V-shaped fracture in the interpretative drawing of (A) is outlined by the dashed line. (D) Diagenetic fractures (some arrowed) in the 10th vertebra of PIMUZ T 2819. (E) Fractures on the 5th vertebra of PIMUZ T 2819 previously interpreted as bite traces by Wild^{S28, S29}; white arrows mark the diagenetic cracks running through the slab, one of which bifurcates from the other just across a small unidentified bone fragment (black arrowhead, previously interpreted as the bitten off portion of the 5th vertebra by Wild^{S28}), note that the largest crack (that on the left) runs through and displaces the posterior part of the 4th vertebra; white arrowheads mark notches on both the bone (magnified in bottom left of (E)) and the sedimentary matrix that were likely produced during excavation or preparation of the specimen.



Figure S2. Artistic rendition of the decapitation scene of *T. hydroides* by one of several possible perpetrators, *Nothosaurus giganteus*. The predator is attacking the prey from its rear and above, as inferred from PIMUZ T 2819, in a shallow marine environment. A smaller *T. longobardicus* swims away from the scene, as well as a shoal of ray-finned fish. Image credit: Roc Olivé / Institut Català de Paleontologia Miquel Crusafont.

Resources Availability

Lead contact

Further information and requests for resources and reagents should be directed to and will be fulfilled by the lead contact, Stephan N. F. Spiekman (stephanspiekman@gmail.com)

Materials, and Data and code availability

This study did not generate new unique reagents. The digital models of PIMUZ T 2819 and PIMUZ T 3901 are publicly accessible through *figshare* (<https://figshare.com/>): DOI for PIMUZ T 2819, 10.6084/m9.figshare.22591657; DOI for PIMUZ T 3901, 10.6084/m9.figshare.22591660.

Supplemental Methods

Both *Tanystropheus* specimens derive from the Middle Triassic marine fossil lagerstätte of Monte San Giorgio (Ticino, Switzerland) and are stored at the Paläontologisches Institut und Museum der Universität Zürich, Switzerland (PIMUZ). Decapitation was established in PIMUZ T 2819 (*T. hydroides*, Besano Formation; Figure 1A) and PIMUZ T 3901 (*T. longobardicus*, Cassina Beds, Meride Limestone; Figure 1B)^{S1,S2}. Lighting in different orientations, hand lenses and a dissecting microscope were used to analyze the specimens. Three-dimensional (3D) photogrammetric models of the broken vertebra and ribs of each specimen were generated mainly following the workflow of Mujal et al.^{S3}, using the following software: Agisoft Metashape (Professional edition, educational version) v.1.8.3 to generate the mesh and texture from the photographs taken with a Canon PowerShot SX410 IS; MeshLab v.2020.07 to clean, scale and orientate the mesh; ParaView v.4.1.0 to create false color depth maps and contours in order to aid identification of features. The 3D models of the two specimens are publicly accessible through *figshare* (<https://figshare.com/>): DOI for PIMUZ T 2819, 10.6084/m9.figshare.22591657; DOI for PIMUZ T 3901, 10.6084/m9.figshare.22591660.

Nomenclature of bite traces is primarily based on^{S4}, with further input from^{S5-S20} for their interpretation and implications for feeding behavior. Terminology and interpretation of bone fractures follow^{S21-S23}. Identification of taphonomic features (postmortem modification of preserved remains, including opisthotonus) follows^{S24-S27}.

Supplemental Results

Additional description of bite traces

In PIMUZ T 2819 fractures on the 10th cervical vertebra and associated ribs are aligned, drawing a line oblique with respect to the neck axis (Figure 1A, C). The exposed lateral surface of the last vertebra displays a V-shaped bone splinter (*sensu*^{S21}) that has collapsed within the hollow centrum and which is slightly displaced inwards and backwards; its acute end points anteriorly (Figure 1C, D; Figure S1A). The anteriormost area of this fractured portion displays a straight score (*sensu*^{S4}) widening backwards (Figure 1D, E). An oval-shaped depression ~3 mm deep is present within the lower branch of the V-shaped fracture (Figure 1D; Figure S1A). Around this puncture (*sensu*^{S4}) the bone is partially plastically deformed, as occurs in fresh bones^{S21-S23}. Anterior to the puncture, following the lower branch, the bone is pushed in with a vertical straight fracture as a result of the pressure caused by the bite (Figure 1D). In the upper branch the bone is broken in a roughly oval-shape outline and slightly deformed, representing another puncture (Figure 1D). The distance between the punctures is 14.5 mm. The posterior cervical vertebrae are tightly articulated,

forming a gentle curved line indicative of limited decay prior to burial (see description of taphonomy below). The limited number of bite traces and minimal scattering of elements are both features that argue against scavenging as the cause of the decapitation^{S5, S6, S11, S13-S16, S19, S20}. In addition, deep, penetrative punctures that completely pierce the bone, as those observed on PIMUZ T 2819 (i.e. bites causing severe trauma on prey: Figure 1D; Figure S1A) are commonly associated with predatory behaviors^{S8, S12, S17-S20}, particularly when combined with the abovementioned limited bite traces and minimal bone scattering^{S11}.

The 7th cervical vertebra of PIMUZ T 3901 preserves its anteriormost part mostly intact, including the articulations with the ribs (Figure 1B, F; Figure S1B). The rest of the vertebra is missing, except for a roughly rectangular portion of the right side. All broken margins are irregular with acute angles, displaying smoothed cross section surfaces (Figure 1F; Figure S1B), clearly corresponding to spiral fractures (*sensu*^{S23}). Such fracturing is consistent with that inflicted by predators and scavengers^{S9, S11, S14, S15, S20, S21}. In the top posterior part of the 5th vertebra an oval pit (*sensu*^{S4}) is present (Figure 1G; Figure S1C). It is defined by clean concentric fractures that accommodate the slightly depressed bone (Figure S1C). Notably, the cervical ribs directly associated with this vertebra are broken (Figure 1H), differing from all the rest, which are still in place. Furthermore, the distal end of the shaft of another rib is broken at the same anteroposterior level as the vertebral pit (Figure 1H). As in PIMUZ T 2819, the reduced number of bite traces, being mostly associated with the breakage of the vertebra, together with the high degree of articulation of the vertebrae and ribs favor the interpretation of a predatory behavior rather than scavenging^{S5, S9, S11, S13, S14, S16, S18-S20}.

Comparison of types of bone fractures

The fractures directly associated with the severing of the broken vertebra display smooth surfaces, without shattering (*sensu*^{S21}) of the surrounding bone, in both *Tanystropheus* specimens. Shattering around the fractures occurs when the bone structure is brittle and would indicate that the fractures occurred when the bone was already dry (i.e. in the postmortem period, a considerable time after death, see^{S21-S24}). Instead, the fractures of the last vertebra preserved in each *Tanystropheus* specimen are oblique and spiraled and the broken surface is smoothed in cross section; those fractures typically occur on wet or fresh bones in the perimortem period^{S21-S23}. Other regions of the preserved vertebrae display another type of fracturing, corresponding to numerous braided cracks (Figure S1D) that likely originated due to compaction and compression of the bones during diagenesis. These cracks mainly occur on curved surfaces, which are more prone to being fractured due to compaction and compression when embedded in softer material (i.e. in fine-grained sediments). Notably, these cracks differ from crumbling, cracking and flaking of the cortical

bone that occurs due to weathering under subaerial exposure prior to burial^{S24}, features otherwise not observed in the studied specimens (see main text and text below).

Three prominent, post-sedimentary cracks in the matrix run through the preserved cervical column of PIMUZ T 2819; through the posterior end of the 4th vertebra, the middle section of the 7th vertebra, and the articulation of the 9th and 10th vertebrae, respectively (Figure 1A). The first crack is the result of sedimentary faulting, whereas the middle and posteriormost post-sedimentary cracks are either the result of faulting or occurred during excavation or transport of the specimen. The crack unambiguously resulting from faulting bifurcates just above the articulation of the 4th and 5th vertebrae, and a small piece of bone, likely coming from the same specimen, is present within the fractured sedimentary matrix (Figure S1E). Although the origin of the isolated small bone fragment and the missing portion of bone from the 5th vertebra cannot be confidently assessed, any relation to predation and scavenging can be excluded (see below). In PIMUZ T 3901 only a single post-sedimentary crack runs through the cervical column, at the anterior end of the 3rd vertebra (Figure 1B). None of the post-sedimentary cracks in either specimen are related with the bone fractures that are considered to be perimortem here.

Previous interpretations and taphonomy

Bite traces on PIMUZ T 2819 were previously briefly reported on by Wild (^{S28}, p. 146; ^{S29}, p. 20). The bite traces identified in the present study that are directly associated with the severed 10th vertebra were not identified by Wild. Instead, he identified several notches on the margin of a small broken portion of the anterior end of the neural spine on the 5th vertebra as bite traces (Figure S1E). It was suggested that they were inflicted by a large predator and that as a possible consequence of this trauma on the 5th vertebra the neck broke at the 10th vertebra. In the present reevaluation of these features on the 5th vertebra (Figure S1B), no distinct perimortem notches could be observed. Instead, the bite traces inferred by Wild likely result from preparation or excavation, since they clearly show fracturing of a diagenetically crystallized bone (as described above, for comparison see Figure S1D). This interpretation is supported by the presence of numerous, additional pits present in the adjacent region of the slab that were clearly generated with preparation or excavation tools. These pits on the sediment and the broken neural spine of the 5th vertebra together form a subcircular outline and both display a similar size and shape (Figure S1E). The missing portion of bone on the 5th vertebra might have been lost during preparation or the excavation process of the specimen. Alternatively, this portion of bone could also have been lost during the post-sedimentary fracturing/faulting of this portion of the slab. Even when the preparation marks on the sediment are not considered, it seems extremely unlikely that a bite on the edge of the neural spine of the 5th

cervical vertebra would produce enough force to break the neck over 1 m away at the posterior end of the 10th vertebra. Furthermore, all other elements remain undisrupted (as would be the case in scavenging, see references above) and the curvature of the neck related to opisthotonus (see below) is continuous along the preserved vertebral column, whereas it would reasonably be expected to have been interrupted in this region if massive portions of the dorsal musculature and ligament would have been ripped away^{S25}.

Wild also suggested that the bite traces in PIMUZ T 2819 were the result of terrestrial scavenging prior to the transportation of the specimen to its final marine deposition. This was based on the continuous dorsal flexure of the neck in this specimen (Figure 1A), as well as in other specimens of *Tanystropheus* (also present in PIMUZ T 3901; Figure 1B), also known as opisthotonus, which was interpreted by Wild as resulting from desiccation of the muscles and ligaments in a terrestrial environment (^{S28}, p.144-146). Although the cause of opisthotonic posture in tetrapods remains ambiguous (e.g.^{S25-S27}), it certainly also occurs in water. Opisthotonus to a similar extent as seen in the neck of *Tanystropheus* is also observed in unambiguously marine reptiles, including long-necked plesiosaurs (e.g.^{S30}) and it therefore does not represent evidence that PIMUZ T 2819 was preyed upon on land. As outlined above, the bone surfaces also lack any evidence of subaerial weathering, as expected for terrestrial desiccation^{S24}.

The break of the neck of PIMUZ T 3901 was also briefly treated by Wild (^{S31}, p. 8), who considered that it occurred prior to burial, but that the specimen did not possess bite traces, in contrast to PIMUZ T 2819. However, a tooth-derived, unhealed pit (defined by concentric fractures) on the 5th vertebra can clearly be discerned (Figure 1G; Figure S1C), suggesting that this specimen was also preyed upon.

The skull of PIMUZ T 2819 is heavily diagenetically crushed dorsoventrally and partially disarticulated, and it has been somewhat displaced relative to the cervical column (Figure 1A). The anterior half of the preserved neck of PIMUZ T 2819 is also slightly disarticulated, as is indicated by the relatively large angles formed between the individual vertebrae and the displacement of the cervical ribs from their associated vertebrae. In the posterior portion of the preserved neck the vertebrae have a gradual, continuous curvature and the ribs form a tight bundle that is oriented parallel and positioned directly ventral to the vertebrae, corresponding to the inferred in vivo configuration of the neck^{S32}. Only the final, broken vertebra deviates from this line. It is slightly oriented ventrally with respect to the previous vertebra, suggesting limited decay or a displacement that is the direct result from the impact of the predator. The latter interpretation might be supported by the fact that the head of one of the ribs of the severed vertebra is broken and displaced, suggesting some sort of disruption of this portion of the neck. Therefore, the soft tissue of

the anterior half of the specimen was clearly in the process of decomposition prior to fossilization, whereas decay was more restricted in the posterior section. Although its skull is fully articulated with the cervical column, PIMUZ T 3901 also exhibits some evidence of soft tissue decomposition based on the disarticulation of the ribs from the corresponding vertebrae in the posterior section of the preserved neck (Figure 1B). Decomposition in both specimens took place after decapitation, which occurred in the perimortem phase and thus prior to decay, as indicated by the wet or fresh bone fractures of the severed vertebrae in both specimens (see main text and text above).

Supplemental References

- S1. Spiekman, S.N.F., and Scheyer, T.M. (2019). A taxonomic revision of the genus *Tanystropheus* (Archosauromorpha, Tanystropheidae). *Palaeontologia Electronica* 22, 1-46.
- S2. Stockar, R. (2010). Facies, depositional environment, and palaeoecology of the Middle Triassic Cassina beds (Meride Limestone, Monte San Giorgio, Switzerland). *Swiss Journal of Geosciences* 103, 101-119.
- S3. Mujal, E., Marchetti, L., Schoch, R.R., and Fortuny, J. (2020). Upper Paleozoic to lower Mesozoic tetrapod ichnology revisited: Photogrammetry and relative depth pattern inferences on functional prevalence of autopodia. *Frontiers in Earth Science* 8, 248.
- S4. Binford, L.R. (1981). *Bones: ancient men and modern myths*, (San Diego, California, USA: Academic press).
- S5. Blumenschine, R.J. (1986). Carcass consumption sequences and the archaeological distinction of scavenging and hunting. *Journal of Human Evolution* 15, 639-659.
- S6. Shipman, P. (1986). Scavenging or hunting in early hominids: theoretical framework and tests. *American Anthropologist* 88, 27-43.
- S7. Davidson, I., and Solomon, S. (1990). Was OH7 the victim of a crocodile attack? In *Problem Solving in Taphonomy: Archaeological and Palaeontological Studies from Europe, Africa and Oceania*, S. Solomon, I. Davidson and D. Watson, eds. (St. Lucia, Queensland, Australia : Anthropology Museum, University of Queensland: Tempus), pp. 197-206.
- S8. Carpenter, K. (1998). Evidence of predatory behavior by carnivorous dinosaurs. *Gaia* 15, 135-144.
- S9. Njau, J.K., and Blumenschine, R.J. (2006). A diagnosis of crocodile feeding traces on larger mammal bone, with fossil examples from the Plio-Pleistocene Olduvai Basin, Tanzania. *Journal of Human Evolution* 50, 142-162.
- S10. D'Amore, D.C., and Blumenschine, R.J. (2009). Komodo monitor (*Varanus komodoensis*) feeding behavior and dental function reflected through tooth marks on bone surfaces, and the application to ziphodont paleobiology. *Paleobiology* 35, 525-552.
- S11. Fiorelli, L.E. (2010). Predation bite-marks on a peirosaurid crocodyliform from the Upper Cretaceous of Neuquén Province, Argentina. *Ameghiniana* 47, 387-400.
- S12. Hone, D.W., and Rauhut, O.W. (2010). Feeding behaviour and bone utilization by theropod dinosaurs. *Lethaia* 43, 232-244.
- S13. Longrich, N.R., Horner, J.R., Erickson, G.M., and Currie, P.J. (2010). Cannibalism in *Tyrannosaurus rex*. *PLoS One* 5, e13419.
- S14. Drumheller, S.K., and Brochu, C.A. (2014). A diagnosis of *Alligator mississippiensis* bite marks with comparisons to existing crocodylian datasets. *Ichnos* 21, 131-146.

- 365 S15. Drumheller, S.K., and Brochu, C.A. (2016). Phylogenetic taphonomy: A statistical and
366 phylogenetic approach for exploring taphonomic patterns in the fossil record using
367 crocodylians. *Palaaios* 31, 463-478.
- 368 S16. Drumheller, S.K., McHugh, J.B., Kane, M., Riedel, A., and D'Amore, D.C. (2020). High
369 frequencies of theropod bite marks provide evidence for feeding, scavenging, and possible
370 cannibalism in a stressed Late Jurassic ecosystem. *PLoS One* 15, e0233115.
- 371 S17. Drumheller, S.K., Stocker, M.R., and Nesbitt, S.J. (2014). Direct evidence of trophic
372 interactions among apex predators in the Late Triassic of western North America.
373 *Naturwissenschaften* 101, 975-987.
- 374 S18. Pujos, F., and Salas-Gismondi, R. (2020). Predation of the giant Miocene caiman *Purussaurus*
375 on a mylodontid ground sloth in the wetlands of proto-Amazonia. *Biology Letters* 16,
376 20200239.
- 377 S19. Hone, D.W., and Watabe, M. (2010). New information on scavenging and selective feeding
378 behaviour of tyrannosaurids. *Acta Palaeontologica Polonica* 55, 627-634.
- 379 S20. Mujal, E., Foth, C., Maxwell, E.E., Seegis, D., and Schoch, R.R. (2022). Feeding habits of the
380 Middle Triassic pseudosuchian *Batrachotomus kupferzellensis* from Germany and
381 palaeoecological implications for archosaurs. *Palaeontology* 65, e12597.
- 382 S21. Green, A.E., and Schultz, J.J. (2017). An examination of the transition of fracture
383 characteristics in long bones from fresh to dry in central Florida: evaluating the timing of
384 injury. *Journal of forensic sciences* 62, 282-291.
- 385 S22. Haynes, G., Krasinski, K., and Wojtal, P. (2020). Elephant bone breakage and surface marks
386 made by trampling elephants: Implications for interpretations of marked and broken
387 *Mammuthus* spp. bones. *Journal of Archaeological Science: Reports* 33, 102491.
- 388 S23. Haynes, G. (1983). Frequencies of spiral and green-bone fractures on ungulate limb bones in
389 modern surface assemblages. *American Antiquity* 48, 102-114.
- 390 S24. Behrensmeyer, A.K. (1978). Taphonomic and ecologic information from bone weathering.
391 *Paleobiology* 4, 150-162.
- 392 S25. Faux, C.M., and Padian, K. (2007). The opisthotonic posture of vertebrate skeletons:
393 postmortem contraction or death throes? *Paleobiology* 33, 201-226.
- 394 S26. Cutler, A., Britt, B., Scheetz, R., and Cotton, J. (2011). The opisthotonic death pose as a
395 function of muscle tone and aqueous immersion. In *Journal of Vertebrate Paleontology*,
396 Volume 31. (SOC VERTEBRATE PALEONTOLOGY 60 REVERE DR, STE 500, NORTHBROOK, IL
397 60062 USA), pp. 95-95.
- 398 S27. Reisdorf, A.G., and Wuttke, M. (2012). Re-evaluating Moodie's opisthotonic-posture
399 hypothesis in fossil vertebrates part I: reptiles—the taphonomy of the bipedal dinosaurs
400 *Compsognathus longipes* and *Juravenator starki* from the Solnhofen Archipelago (Jurassic,
401 Germany). *Palaeobiodiversity and palaeoenvironments* 92, 119-168.
- 402 S28. Wild, R. (1973). Die Triasfauna der Tessiner Kalkalpen XXII. *Tanystropheus longobardicus*
403 (Bassani) (Neue Ergebnisse). *Schweizerische Paläontologische Abhandlungen* 95, 1-162.
- 404 S29. Wild, R. (1976). Neues über den Giraffenthalssaurier *Tanystropheus*. *Natur und Museum* 106,
405 13-22.
- 406 S30. Williston, S.W. (1889). A new plesiosaur from the Niobrara Cretaceous of Kansas. In
407 *Transactions of the Annual Meetings of the Kansas Academy of Science*, Volume 12. (JSTOR),
408 pp. 174-178.
- 409 S31. Wild, R. (1980). Neue Funde von *Tanystropheus* (Reptilia, Squamata). *Schweizerische*
410 *Paläontologische Abhandlungen* 102, 1-43.
- 411 S32. Tschanz, K. (1986). Funktionelle Anatomie der Halswirbelsäule von *Tanystropheus*
412 *longobardicus* (Bassani) aus der Trias (Anis/Ladin) des Monte San Giorgio (Tessin) auf der
413 Basis vergleichend morphologischer Untersuchungen an der Halsmuskulatur rezenter
414 Echsen. PhD thesis Universität Zürich.